Article

Exploring New Parameters to Advance Surface Roughness Prediction in Grinding Processes for the Enhancement of Automated Machining

Mohammadjafar Hadad [1,2,*], **Samareh Attarsharghi** [3,*], **Mohsen Dehghanpour Abyaneh** [2], **Parviz Narimani** [2], **Javad Makarian** [2], **Alireza Saberi** [2] **and Amir Alinaghizadeh** [4]

1   Department of Mechanical Engineering, School of Engineering and Technology, University of Doha for Science and Technology, Doha P.O. Box 24449, Qatar
2   School of Mechanical Engineering, College of Engineering, University of Tehran, Tehran P.O. Box 14155-6619, Iran; dehghanpoor.1376@ut.ac.ir (M.D.A.); parviz.narimani@ut.ac.ir (P.N.); makarian.javad@ut.ac.ir (J.M.); saberi.garakani.a@ut.ac.ir (A.S.)
3   Department of Electrical Engineering, School of Engineering and Technology, University of Doha for Science and Technology, Doha P.O. Box 24449, Qatar
4   Institute of Precision Machining (KSF), Furtwangen University, 78532 Tuttlingen, Germany; amir.alinaghizadeh.abiazani@hfu.eu
*   Correspondence: mjhadad@ut.ac.ir or mohammadjafar.hadad@udst.edu.qa (M.H.); samareh.attarsharghi@udst.edu.qa (S.A.)

Abstract: Extensive research in smart manufacturing and industrial grinding has targeted the enhancement of surface roughness for diverse materials including Inconel alloy. Recent studies have concentrated on the development of neural networks, as a subcategory of machine learning techniques, to predict non-linear roughness behavior in relation to various parameters. Nonetheless, this study introduces a novel set of parameters that have previously been unexplored, contributing to the advancement of surface roughness prediction for the grinding of Inconel 738 superalloy considering the effects of dressing and grinding parameters. Hence, the current study encompasses the utilization of a deep artificial neural network to forecast roughness. This implementation leverages an extensive dataset generated in a recent experimental study by the authors. The dataset comprises a multitude of process parameters across diverse conditions, including dressing techniques such as four-edge and single-edge diamond dresser, alongside cooling approaches like minimum quantity lubrication and conventional wet techniques. To evaluate a robust algorithm, a method is devised that involves different networks utilizing various activation functions and neuron sizes to distinguish and select the best architecture for this study. To gauge the accuracy of the methods, mean squared error and absolute accuracy metrics are applied, yielding predictions that fall within acceptable ranges for real-world industrial roughness standards. The model developed in this work has the potential to be integrated with the Industrial Internet of Things to further enhance automated machining.

Keywords: artificial neural network; grinding; Industrial Internet of Things; machine learning; modeling; sustainable manufacturing; surface roughness; superalloys

1. Introduction

In various industrial productions involving different alloys, achieving smooth surfaces at the end of the manufacturing process is challenging, often resulting in less aesthetically pleasing outcomes [1]. Furthermore, the quality of the ground surface holds paramount importance in advanced systems such as high-speed rotational blades, influencing their efficiency [1]. As a finishing step in the production line, the grinding process strives to achieve fine and precise dimensions within microns on the workpiece, while generating the necessary surface roughness [2]. Diverse types of grinding operations exist, varying in terms of wheel shape, workpiece design, and relative tool-workpiece movement [3].

The grinding process entails an intricate geometrical cutting mechanism, shaped by the number and configuration of undefined cutting edges that interact with the workpiece's surface. This complexity results in various parameters describing the process, arising from the intricate interplay between grinding tools and workpieces. In the context of standard tangential surface grinding, crucial parameters encompass the cutting speed (v_c), feed velocity (v_f), depth of cut (a_e), and width of cut (a_p). Cutting speed equals the grinding wheel's rotational speed, while the feed velocity aligns with the feed direction, which can be tangential or axial relative to the grinding wheel. In this regard, tangential feed velocity (v_{ft}) and axial feed velocity (v_{fa}) are defined based on the grinding wheel's n relation to the workpiece. Notably, the ground surface roughness is significantly influenced by the grinding wheel's material [4] and sharpness, particularly the sharpness of its grains. The grinding process can generate excessive heat, which poses risks to the surface of the work material and can induce flaws due to insufficient removal rates and wheel wear. The energy consumed by the process is distributed among the wheel, workpiece, chip, and coolant. Swift heat dissipation from the workpiece is crucial to prevent the formation of high local temperatures and phase transformations, as well as to mitigate elevated residual temperatures post-grinding. To address this, an effective cooling approach, such as dry methods or lubricating fluids, coupled with the careful selection of process parameters, can curtail heat generation. The choice of appropriate cooling agents is of utmost importance, considering their varied biological, physical, and chemical properties. Some coolants possess environmental hazards and contain chemical compounds that necessitate post-process refinement. Typically, three primary cooling resources are employed in the industry: air, water, and oil. However, optimal cooling strategies often involve a combination of these resources in real-world applications [5,6].

1.1. Grinding of Inconel Alloy

The term Inconel serves as a trademark encompassing a diverse range of over twenty nickel-based superalloys. The hallmark feature of Inconel alloys lies in their exceptional resistance to a spectrum of challenges, including corrosion, oxidation, carburization, pitting, crevice corrosion, and high-temperature strength. These alloys find extensive application in demanding environments such as chemical and petrochemical equipment, components exposed to high-stress conditions like sea-water, gas turbines, rocket motors/engines, spacecrafts, and nuclear reactors [7]. Among these alloys, Inconel 738 stands out as a vacuum-melted, vacuum-cast, precipitation-hardenable nickel-based alloy, comprising approximately seventeen distinct constituents. This alloy is further categorized into the high-carbon version, IN-738C, and the low-carbon version, IN-738LC. An overview of some crucial properties of this remarkable superalloy is provided in [8]. The distinctive mechanical and structural properties of superalloys render machining a complex endeavor, necessitating elevated temperatures and specialized cooling approaches. Notably, the hardening phenomena during the machining process introduce alterations to product mechanical structures, leading to increased tool wear and undesired vibrations. Surface roughness, a fundamental material property, exerts a direct influence on fracture, fatigue, corrosion, and creep behaviors. Consequently, the quest for optimal parameters stands as a substantial challenge within the realm of mechanical engineering.

1.2. Neural Networks

The neurobiologists McCulloch and Pitt introduced neural networks to replicate human brain functions through interconnected computational neurons and weighted connections, as outlined in [9]. Artificial neural networks, a subset of machine learning, provide powerful tools rooted in statistics for solving real-world problems. They excel at handling nonlinearity, parallelism, and noise, enabling researchers to approach complex challenges similarly to how the human brain functions. This involves learning from data to predict outcomes. Neural networks consist of various categories, including Artificial

Neural Networks (ANN) [10], often referred to as Feed-Forward Neural Networks, which process inputs sequentially to make predictions (as depicted in Figure 1).
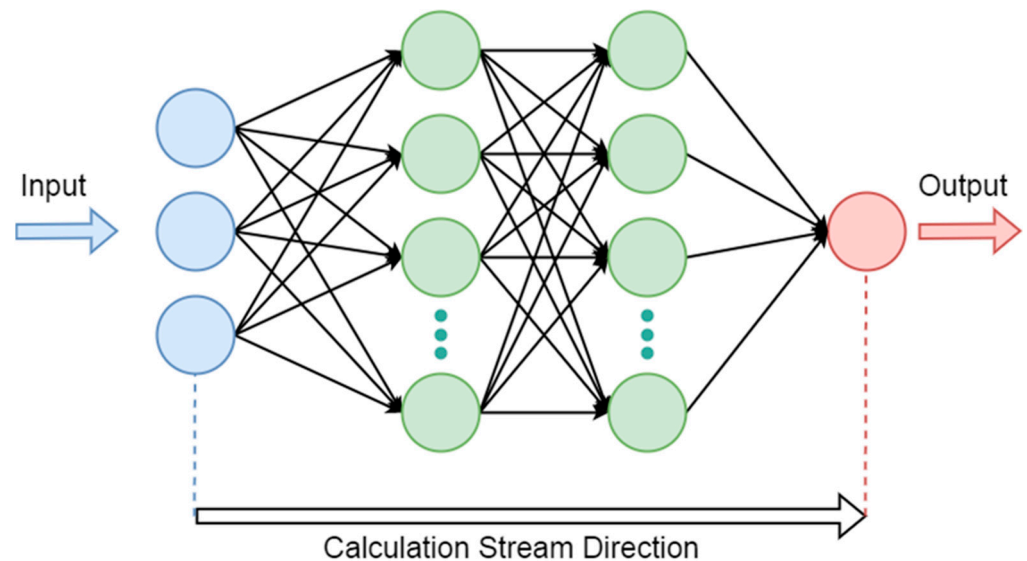

Figure 1. A standard feedforward neural network structure with backpropagation error estimation. This is capable of learning and solving any nonlinear function, and, because of that, this network is popularly known as Universal Function Approximation [10].

1.3. A Literature Review Based on Using NN in the Grinding Process

ANNs find utility in machining and grinding due to their capacity to predict parameter relationships that influence critical outcomes like surface roughness. These processes have an impact across diverse industries [11–14], including aerospace and power generation, where the emphasis lies on optimizing and controlling parameters to achieve improved outcomes. ANNs offer a predictive tool beyond experimental and theoretical analyses, aiding in understanding and controlling complex parameter interactions for improved machining and grinding performance [15–19]. In the realm of grinding procedures for demanding materials like titanium superalloys, it is essential to acknowledge that factors beyond mere roughness measurement hold significance. Temperature control, notably, emerges as a pivotal aspect in this context. Liu et al. employed a backpropagation (BP) neural network using particle swarm optimization to predict high-speed grinding temperatures for titanium matrix composites [15]. The difficulty in machining superalloys like titanium led to the adoption of specialized approaches, such as creep-feed deep grinding (CFDG), influenced by parameters like wheel speed, workpiece velocity, depth of cut, and cooling, which impacts both roughness and grinding force [16]. The study integrated ANN variations to predict grinding forces for titanium machining, aiming for improved results [14]. In the case of hybrid machining processes (HMPs), which combine electrical discharge machining (EDM) and grinding, the authors in [17] investigated hybrid parameters affecting material removal rate and surface roughness using ANN and RSM, leveraging different tests. The complexity of grinding nature necessitates a demanding optimization of prediction methods, where BP neural networks offer potential for automatic optimization by establishing relationships between processing parameters and surface roughness, addressing the intricate physical mechanisms involved in industrial grinding [18]. In [19], the authors introduced a technique employing the radial basis function (RBF) to tackle the issue of unevenly distributed abrasive particles in belt grinding procedures. Likewise, ANNs have been employed for surface roughness prediction in studies [20–28], yet cooling methods [29,30] and dressing parameters [31] have not been treated as distinct variables in the prediction algorithms. Additionally, it is important for the dataset size to be sufficiently large, which has not been consistently observed in the literature. Furthermore, in the domain of grinding, proficient neural network implementation should encompass various

sizes and transfer functions [32–34]. Addressing the gaps in the current literature, this study utilizes ANNs with a substantial dataset [15–19,35,36], varying sizes, and transfer functions. In this study, cooling methods and dressing parameters are also considered as independent factors and are quantified for the modeling and prediction of surface roughness, which was not considered in the previous works. One of the most promising aspects of this model lies in its compatibility with the Industrial Internet of Things (IIoT). When this model is smoothly integrated with the IIoT infrastructure, a higher level of innovation and efficiency in digital manufacturing processes can be realized. Through this integration, access to a valuable stream of real-time data is facilitated, enabling the monitoring, analysis, and optimization of machining operations to a greater extent than previously achievable.

This study explores the impact of industrial grinding process parameters on surface roughness, comparing MQL and conventional cooling methods. It employs a range of parameters, including various dressing depths, tool feed rates, and stationary dresser types, to establish the grinding wheel cycle on an Inconel 738 superalloy workpiece. The research emphasizes the substantial influence of the dresser and cooling method on surface roughness and acknowledges the complexity of this relationship. It introduces the novel approach of treating cooling methods and dressers as independent parameters, enhancing accuracy and introducing complexity. This study also presents a sophisticated algorithm for optimizing the ANN structure, indicating the ideal network configuration for the dataset. The ANN algorithm is found to be versatile and suitable for online deployment and broader applications across engineering domains.

The rest of this paper is organized as follows. The experimental setup is explained in Section 1 followed by the methodology of implementing ANNs in Section 3. The results of applying the ANNs are discussed in the following sections.

2. Experimental Setup

A prompt 300–1000 grinding machine (Taichung City, Taiwan) was utilized to conduct the experiments in this study (Figure 2). The workpiece material was Inconel 738 with dimensions of $200 \times 40 \times 16$ mm. Dressing tools included both single-edge and for-edge diamond dressers with access angles of ($\alpha = 10°$). The grinding wheel, Al_2O_3 (WA60K9V) type, maintained a constant peripheral speed (cutting speed) of 47 m/s and a 450 mm diameter (Figure 2). The depth of cut during the grinding of specimens was fixed at 10 μm. Prior to each experiment, the grinding wheel underwent three dressing cycles with varying dressing conditions, which are also detailed in Table 1. Cooling methods, crucial for workpiece quality in industrial settings, were implemented using two approaches [37]. The conventional wet machining technique employed a 5% concentration of water-miscible coolant lubricant at a flow rate of 4 L/min. Minimum quantity lubricant (MQL) involved a handmade system controlling a constant flow rate of 200 mL/h of vegetable oil, utilizing the Venturi effect to mix air and oil. Surface roughness was measured for each condition to determine the coolant's effects on output parameters. The experimental details and conditions are summarized in Tables 1 and 2.

Any prediction method, whether statistical or artificial, relies on data availability. Sufficient data quantity is crucial for results to hold merit across most scenarios, a consideration that some prior publications have neglected regarding the impact of data size on simulation accuracy. In this study, using the experimental setup, a substantial dataset comprising 125 unique conditions and encompassing eight distinct parameters was collected. Five of these parameters were input variables measured prior to the experimental setup, while the remaining three represent mean, maximum, and minimum surface roughness values. Mahr Surf PS1 Model-Germany was used to take multiple precise measurements of surface roughness. This resulted in three data points for dressing depth, which were then used for further analysis. One challenge in implementing the dataset is transforming qualitative parameters into quantitative ones for compatibility with prediction algorithms. Thus, assigning non-zero positive real numbers to each type of qualitative input parameter becomes necessary. In this study, two cooling methods, Wet and MQL, were employed and

designated as numbers 1 and 2, respectively. Similarly, for dressing types, the numbers 1 and 4 correspond to single and four points.
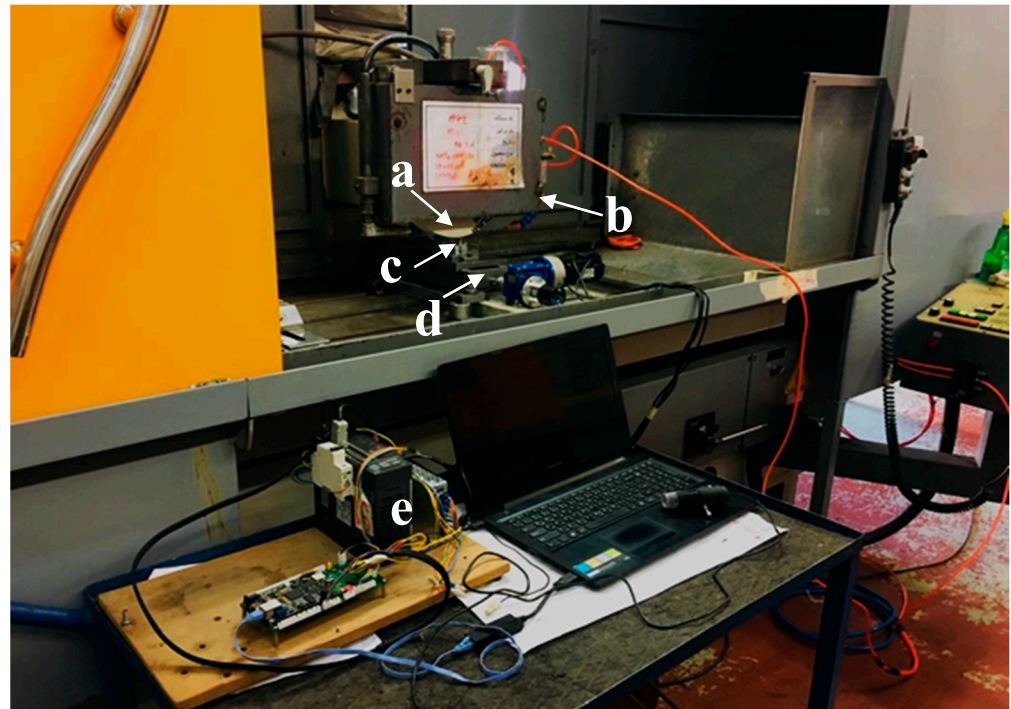

Figure 2. Experimental setup: (a) grinding wheel, (b) coolant–lubricant nozzle, (c) dressing tool, (d) dressing table, and (e) dressing table controller.

Table 1. Fixed parameters during the grinding process [37].

Grinding Elements	Parameters
Grinding Mode	Plunge surface grinding, down cut
Grinding Wheel	Al_2O_3: WA60K9V (ds = 450 mm)
Wheel Speed (v_s)	47 m/s
Depth of Grinding (a_e)	30 μm
Fluid used in grinding with cutting fluid and dressing operation	Water-soluble oil with a concentration of 5%
Cutting fluid flow rate in wet grinding	4 L/min
MQL Oil	Vegetable oil
MQL flow rate	200 mL/h
MQL Viscosity (at 20 °C)	84 cP
MQL Carrier Gas	Compressed air
MQL Gas Pressure	5 bar
Workpiece Material	Nickel-base superalloy-Inconel 738
Workpiece Dimensions	200 mm × 40 mm × 16 mm
Dresser Material	Stationary Diamond
Dresser Type	Single-edge and Four-edge
Dresser Access Angle (α_d)	10°

Table 2. Five input parameters are taken into account, each with multiple values, as illustrated in the provided table. It is noted that according to the literature review, other studies consider lower numbers of parameters [37].

Grinding Variable Parameter	Value
Grinding Feed Rate—Table Speed (v_{ft})	4.5, 15 m/min
Dressing Feed (v_{fd})	50, 85, 213, 420, 600 mm/min
Depth of each dressing pass (a_d)	2, 5, 10, 20 μm
Number of Dressing passes	$N_{dt} = 3$
Cooling Type	Wet; MQL
Stationary Diamond Dresser Type	Single-edge; Four-edge

The dataset for the ANN is collected under the aforementioned experimental conditions and parameters, and a randomly selected set of the gathered data is displayed in Appendix A, Table A1. A comparison of the real surface roughness (R_z) against predicted roughness with ANN is presented in Appendix B, Figure A1, along with the analysis of the ANN test data in Table A2. The influence of tool conditions on the final results is worth highlighting. Therefore, prior to each test, the health of tools (with special attention to the grinding wheel) was inspected, and after each dressing procedure, the examination was reiterated.

3. Methodology

3.1. Networks with Hidden Layers

To process the data and predict the surface roughness, the employed ANN structure as well as accuracy metrics are outlined as follows. In the current study, a neural network with five inputs has been implemented, as illustrated in Figure 3. To fulfill the neural network requirement, qualitative parameters like dressing type and cooling type have also been transformed into quantitative ones. The architecture employed is a feedforward [38,39] neural network featuring one or two hidden layers, which is commonly recognized as a deep-learning network due to its ability to uncover intricate patterns.
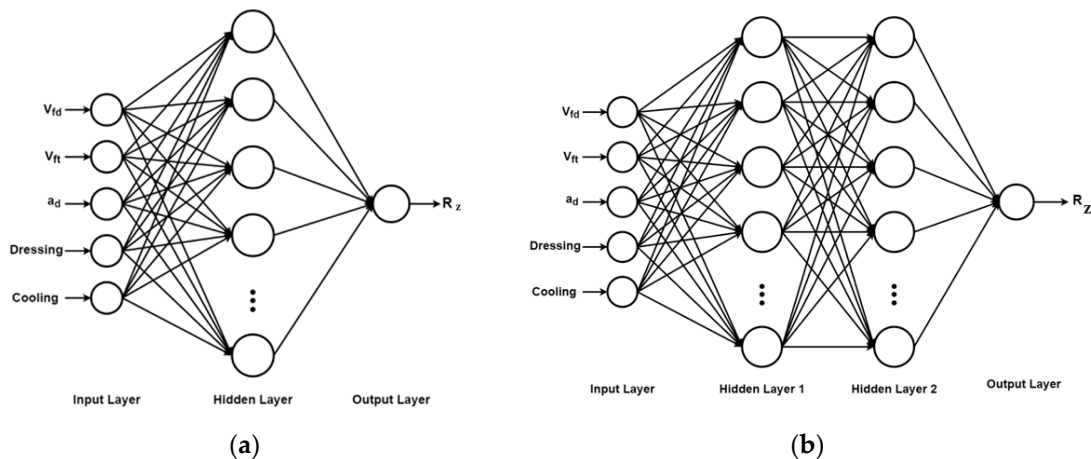

(**a**)
(**b**)

Figure 3. ANN implementation that contains one (**a**) and two hidden layers (**b**) with all properties that are included in the deep network.

The diagram in Figure 4 shows the data preparation, training, and testing process.

3.2. Accuracy Metrics

Accuracy metrics refer to the procedure used to evaluate the machine learning prediction's validity. Selecting an appropriate accuracy metric for assessing a specific prediction

is investigated in [40]. The correlation coefficient (R) and coefficient of determination (R^2) are widely used for the evaluation of the goodness of linear fit of regression models in ANNs [41]. Metrics that rely on absolute errors or squared errors are termed scale-dependent metrics [42]. These metrics maintain the same scale as the initial data, presenting errors in the same units [43]. The comparison of scale-dependent metrics can be challenging when dealing with series of varying scales or units. Despite their lack of unit-free characteristics, scale-dependent metrics are often preferred in machine learning evaluation. Widely used examples include Mean Squared Error (MSE), Root Mean Squared Error (RMSE), and Mean Absolute Error (MAE) [43]. The methods described in this section are applied, in a MATLAB environment, to the dataset achieved by the experimental setup, and the results, including the evaluation of the prediction by the MSE metric, are reported in the following section.
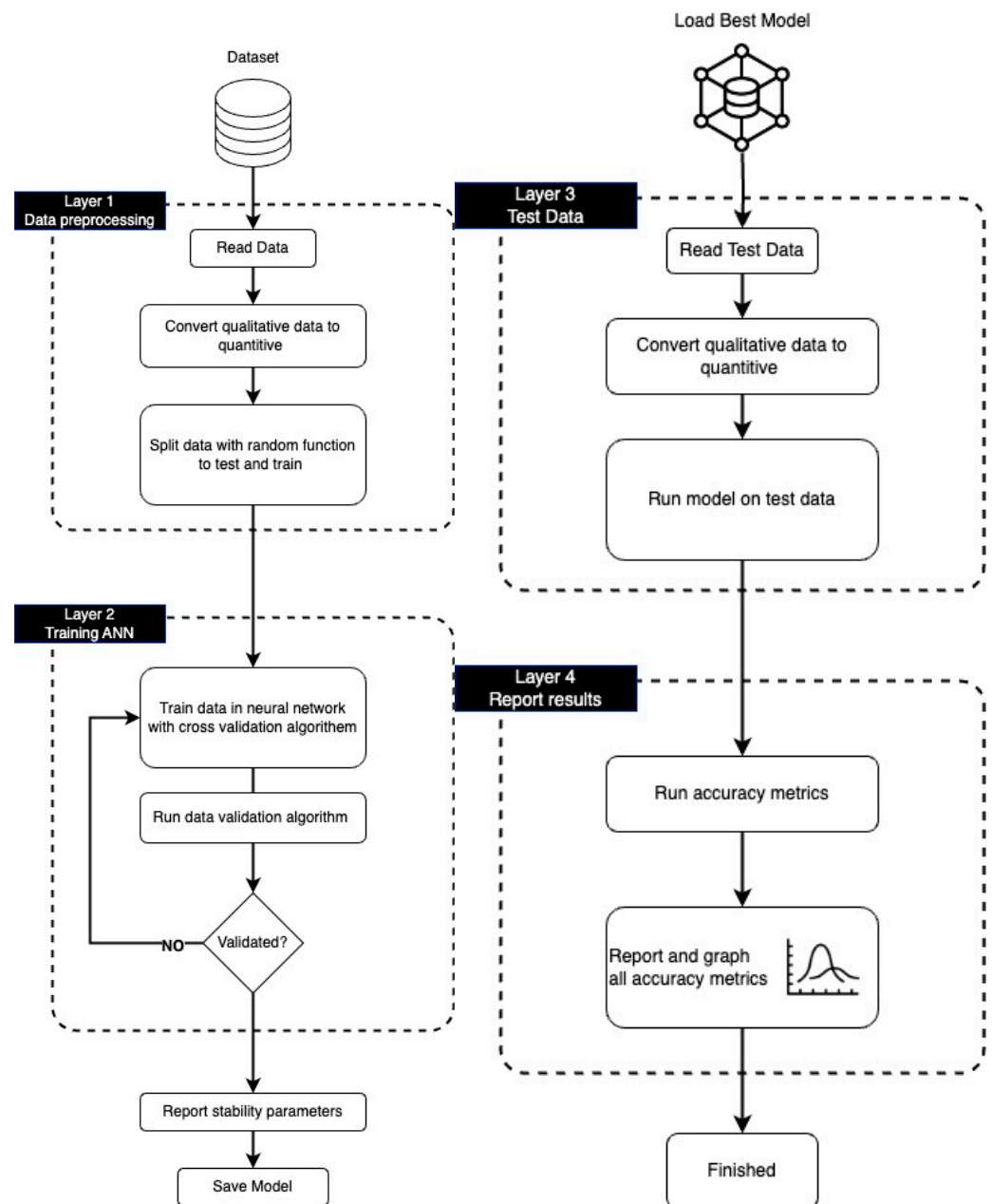

Figure 4. Data preparation, training, and testing.

4. Results and Discussion

4.1. Surface Roughness

Workpiece surface roughness values (Figures 5–7) indicate that the MQL technique in the gridding of Inconel 738 has significant effects on the grinding performance. Notably, in the experimental set up, this is achieved by significantly reducing cutting fluid consumption from 4 L/min to 200 mL/h. On the other hand, by increasing the dressing feed and generating a coarse topography on the grinding wheel surface, the ground workpiece surface roughness is increased. One of the factors increasing the workpiece surface roughness is the penetration of more grains into the workpiece. Increasing the table speed during grinding will result in the penetration of more grains, which is shown in Figures 5–7 for different machining conditions. The experimental results and analysis have been extensively reported in [37], and this article explores the modeling and prediction of surface roughness using artificial neural networks. It is important to mention that in this article, to prevent the model from overfitting during the prediction of surface roughness, the algorithm employs random data selection. Consequently, the parameter values presented in different figures may vary accordingly.
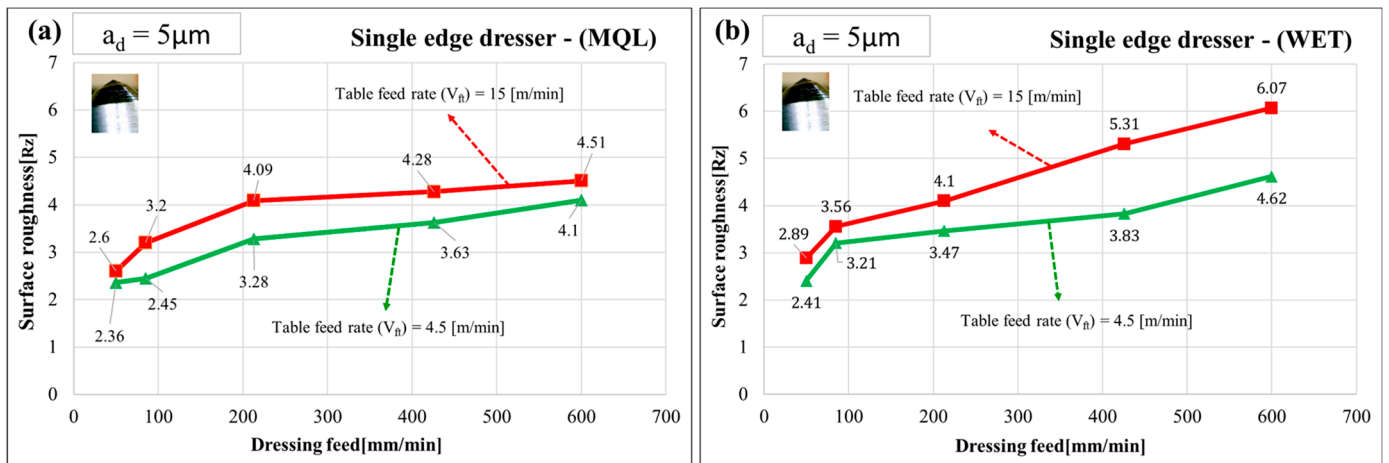

Figure 5. Workpiece surface roughness vs. dressing speed for dressing depth of 5 μm and single-edge dresser after (**a**) MQL grinding and (**b**) wet grinding [37].
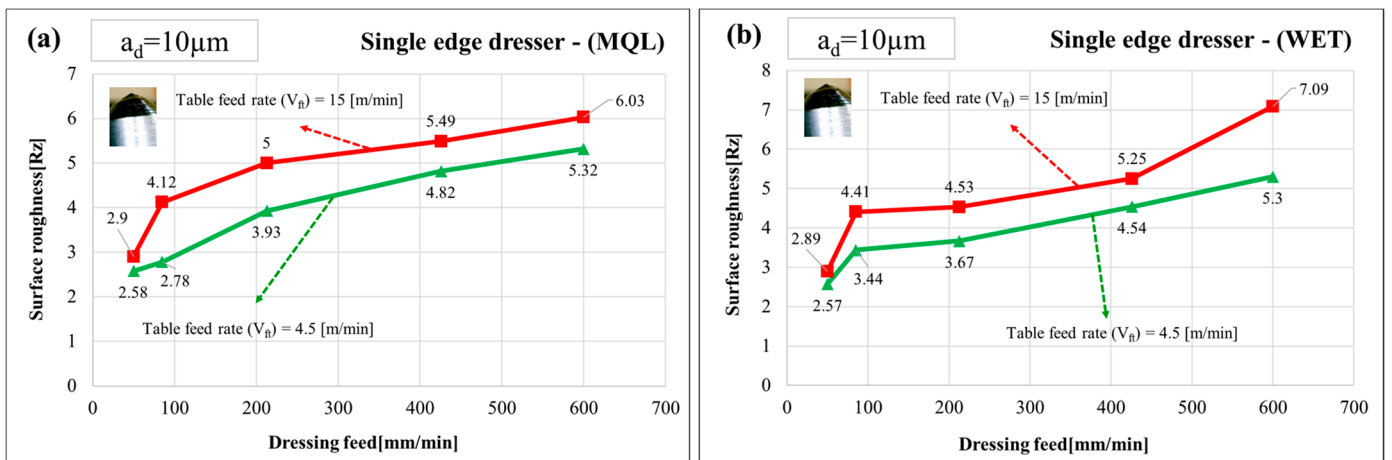

Figure 6. Workpiece surface roughness vs. dressing speed for dressing depth of 10 μm and single-edge dresser after (**a**) MQL grinding and (**b**) wet grinding [37].
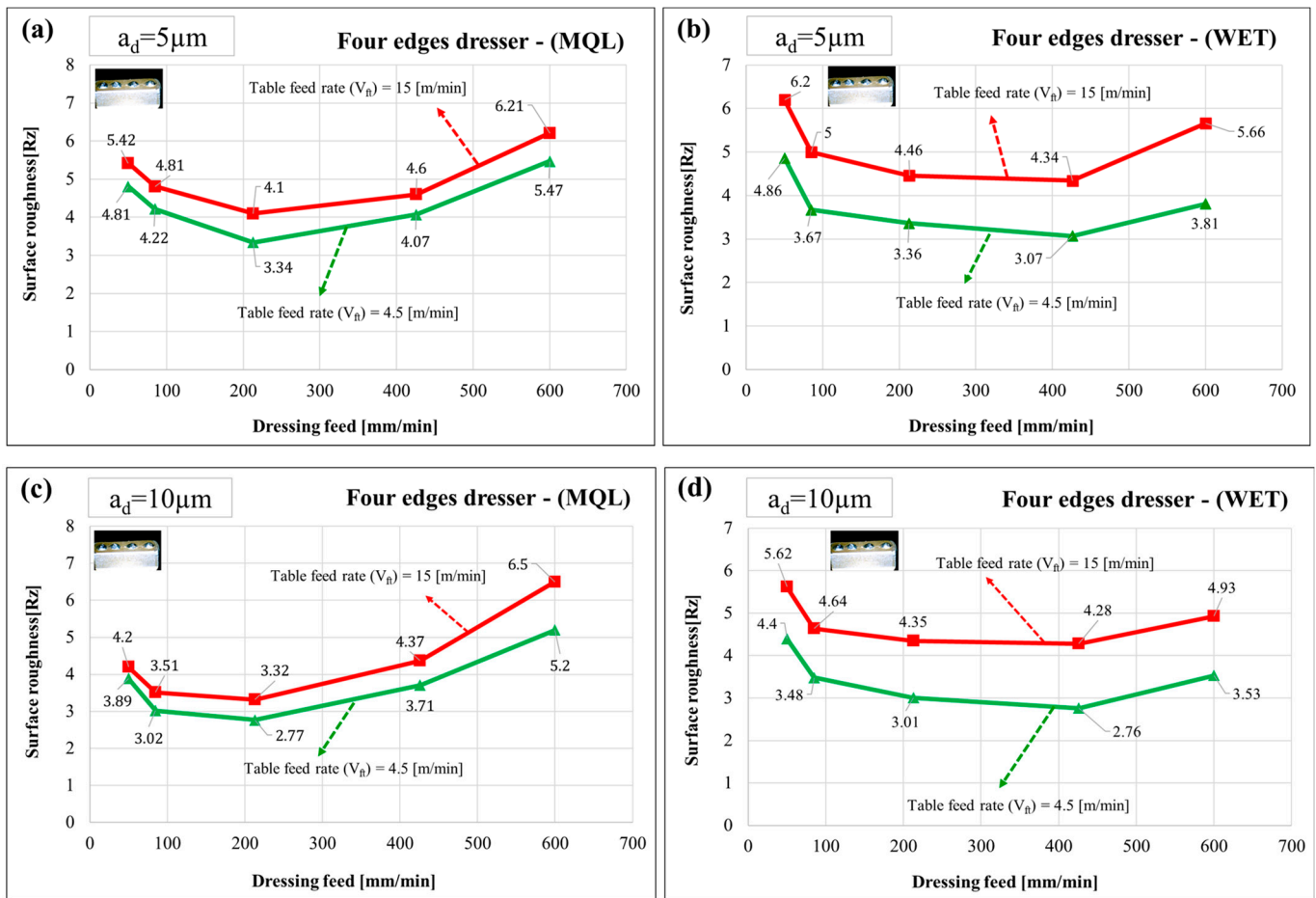
Figure 7. Workpiece surface roughness vs. dressing speed for a dressing depth of 5 μm and four-edge dresser after (**a**) MQL grinding and (**b**) wet grinding; and for a dressing depth of 10 μm and four-edge dresser after (**c**) MQL grinding and (**d**) wet grinding. [37].

4.2. ANOVA

The ANOVA technique was performed to test the adequacy of the established models. The results of fitting the response surface model are presented in Tables 3 and 4. Significance tests for both regression models and individual coefficients, along with a lack-of-fit test, were conducted using Minitab 16 software. The process involved backward elimination to remove nominal model terms, leading to an ANOVA (shown in Table 3) summarizing the significant model terms and quadratic response surface models. Remarkably, the outcomes highlight that beyond key grinding parameters like dresser speed and table speed, the cooling condition also notably impacts the ultimate surface roughness. Table 3 reveals, based on the *p*-values, that three of the examined parameters hold significant importance, both in terms of their physical influence and statistical significance. Table 4 displays the dependance between parameters.

In Table 4, the dresser's dependance on a_d is the most significant and creates the most sensitivity on the surface roughness as the output. Cooling is also dependent on a_d. As the dynamic governing the surface roughness is very complex, analytical approaches and a mathematical model will not show all aspects of it. Therefore, the dependence of all of the parameters cannot be shown by an ANOVA test only, and it may need more complex investigations, which is out of the scope of this work. In the practical approach and experimental setup, surface roughness is shown to be not only sensitive to the parameters proved by ANOVA, but also the remaining parameters in Table 4. Thus, in this study, all of the parameters are chosen for training the model in an ANN.

Table 3. Final results of ANOVA implementation on the current dataset.

Parameter	Sum of Squares (SS)	Degrees of Freedom (DF)	Mean Squares (MS)	F	*p*-Value
Dresser	0.0015	1	0.0015	0.04	0.8506
a_d	0.2283	5	0.0457	1.06	0.386
v_{fd}	0.5124	4	0.1281	2.98	**0.0223**
v_{ft}	0.4784	1	0.4784	11.12	**0.0012**
Cooling	0.7185	1	0.7185	16.7	**0.0001**
Error	4.8199	112	0.0430	-	-
Total	6.7590	124	-	-	-

Table 4. Dependence between the parameters with ANOVA.

Source	Sum Sq.	d.f.	Mean Sq.	F	Prob > F
Dresser	0.00153449	1	0.00153449	0.05395521	0.81694287
a_d	0.22826081	5	0.04565216	1.60520327	0.16889796
v_{fd}	0.51240222	4	0.12810055	4.50422116	0.00255408
v_{ft}	0.47842361	1	0.47842361	16.8221422	0.00010205
Cooling	0.71846775	1	0.71846775	25.2624797	3.24×10^{-6}
Dresser:a_d	0.31042206	3	0.10347402	3.63831266	0.01644337
Dresser:v_{fd}	0.24138786	4	0.06034697	2.12189618	0.08621938
Dresser:v_{ft}	0.06965573	1	0.06965573	2.44920745	0.12173884
Dresser:Cooling	0.0117457	1	0.0117457	0.41299783	0.5223859
a_d:v_{fd}	0.58353194	11	0.05304836	1.86526544	0.05754152
a_d:v_{ft}	0.05313967	3	0.01771322	0.62282532	0.60241049
a_d:*Cooling*	0.45124279	4	0.1128107	3.96660521	0.00561895
v_{fd}:v_{ft}	0.82265751	4	0.20566438	7.23148964	5.46×10^{-5}
v_{fd}:*Cooling*	0.11375702	4	0.02843925	0.99996982	0.41296357
v_{ft}:*Cooling*	0.00087229	1	0.00087229	0.03067123	0.86144164
Error	2.16144852	76	0.02844011		
Total	6.75894998	124			

In Table 4, the dresser's dependency on a_d emerges as the most significant, exerting the highest sensitivity on surface roughness as the output. Cooling also exhibits a dependency on ad. Given the intricate nature of the factors affecting surface roughness, analytical and mathematical approaches might not encompass all aspects of its complexity. Consequently, the reliance of all parameters cannot be exclusively illuminated through ANOVA testing alone, possibly necessitating more intricate investigations beyond the scope of this study. In practical application and experimental setup, surface roughness is demonstrated to be sensitive not solely to parameters confirmed by ANOVA, but also to the remaining parameters outlined in Table 4. As a result, all parameters in the table have been considered for training the ANN model in this study, including the parameters with high *p*-values (such as dresser effect) [44]. This decision was made because a purely statistical analysis, such as ANOVA, may show only some of the correlations but not adequately account for the highly non-linear nature of all of the grinding system parameters, which will indirectly influence the surface roughness.

4.3. ANN Model Implementation

Neurons were trained to determine the best network parameters, including hidden layers, neurons, transfer function layers, and weight values in order to achieve an effective network for modeling the target. Parameters were adjusted to minimize errors during training and testing, and different configurations were evaluated to identify the improved model (Figure 8).
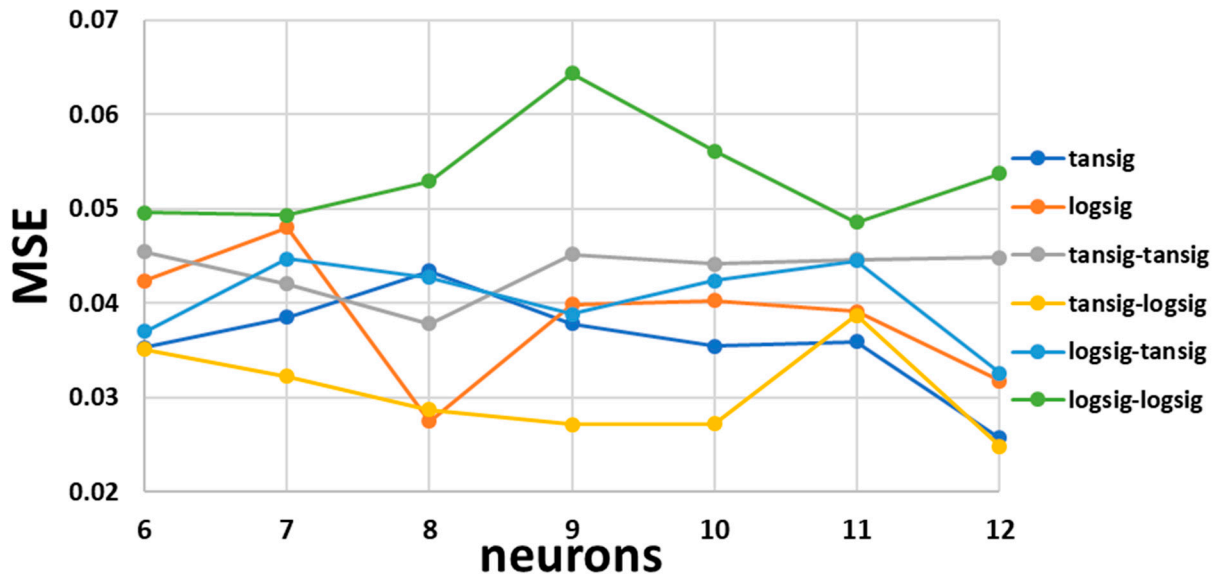

Figure 8. The figure above presents the outcomes of various network implementations. Two network structures were employed, featuring either one hidden layer or two hidden layers. Each hidden layer utilized activation functions such as tansig and logsig, along with varying neuron quantities. The figure showcases the relationship between neuron quantity and Mean Squared Error (MSE), serving as an accuracy metric for the implemented networks.

Ultimately, a network configuration consisting of one input layer, two hidden layers, and one output layer was chosen as the most effective. The highest-performing neuron counts were identified as nine and ten for the hidden layers, while the input and output layers employed four and one neurons, respectively. The transfer functions used between layers are tansig, logsig, and purelin, and the training algorithm employed is trainbr (as shown in Table 5).

Table 5. The overall ANN properties of the current implementation.

Network Configuration			Learning Condition	
Object model		R_z	Learning Scheme	Supervised Learning
	Dresser		Learning rule	Gradient descent
Input neurons	a_d		Hidden neurons	6~20
	v_{ft}		Output neuron	1
Output neuron		R_z	Sample pattern	80% train 10% validation 10% test
Transfer Functions	Purelin Tansig Logsig		Learning rate	0.01
			Marquart adjustment	Mu = 0.05
Training Function	TRAINBR		Max. epoch	1000
Learning Function	LEARNGDM		Goal	0.001

To mitigate overfitting, the data are divided into folds, and accuracy is assessed in each fold. For these datasets, a cross-validation fold value of 5.0 is chosen, determined through iterative experiments to fine-tune the hyperparameters of the selected models. More details of the modeling results are provided in Appendix B.

5. Results and Discussion of NN Implementations

This subsection involves a comparison between the prediction of surface roughness using an ANN and two other methods: Gaussian process regression (GPR) and Regression Trees (RT). This comparison serves to highlight the superior performance of the ANN and the rationale behind its selection for this study. A cross-validation fold value of 5.0 is also implemented in these approaches. The training process encompasses 112 samples obtained from experimental procedures. The results of the chosen features for validation and testing are depicted in Figure 9. The plotted graphs display a comparison between the true and predicted responses of the adopted model. Comprehensive information about these networks is provided in Tables 6 and 7. Both the graphical representations and the tabulated details demonstrate that the ANN offers a superior fit to the data.
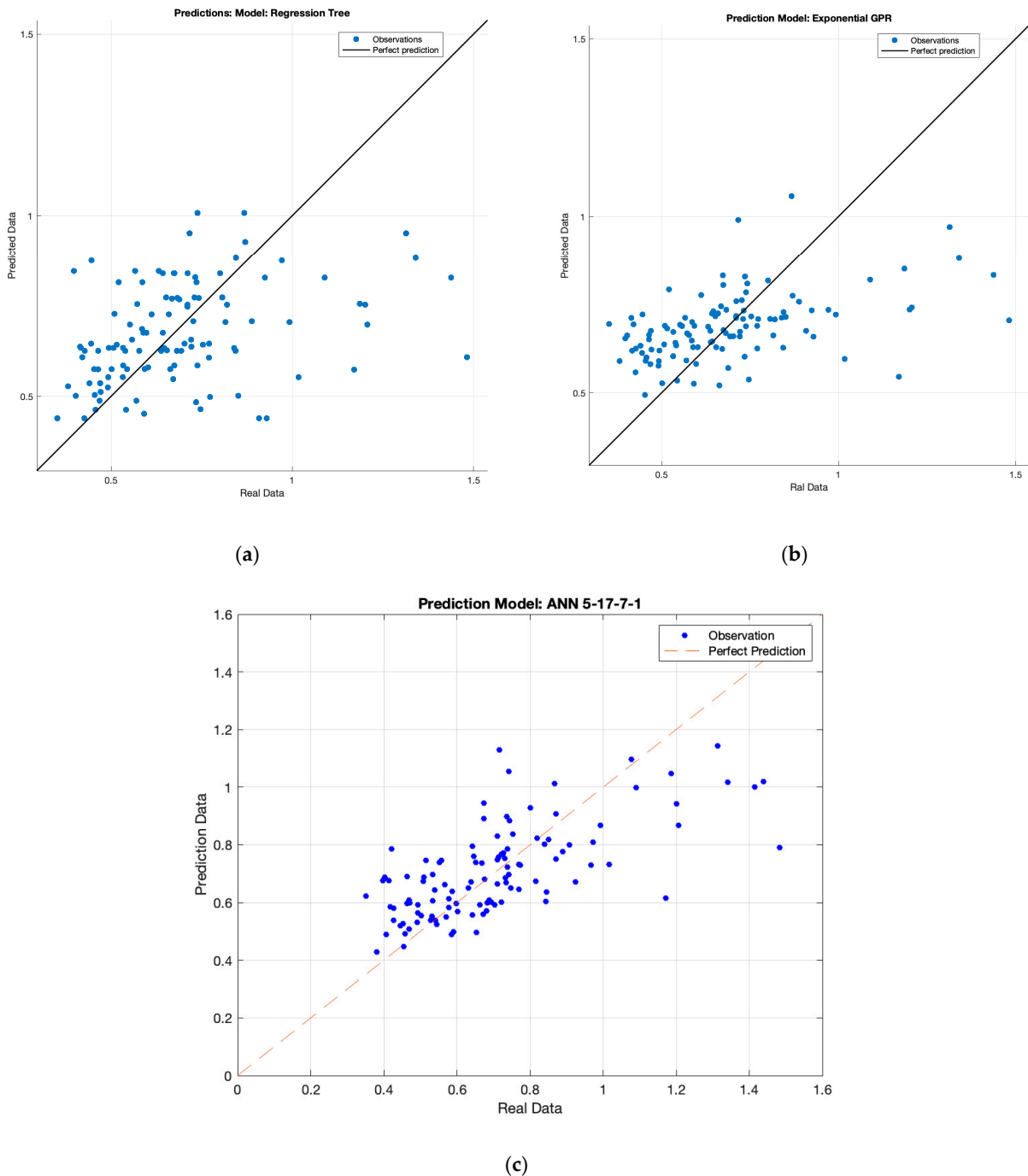

(**a**)

(**b**)

(**c**)

Figure 9. Predicted versus Real date for: (**a**) RT, (**b**) GPR, and (**c**) ANN.

Table 6. Evaluation of the training phase among different algorithms: RT, GPR, and ANN.

Training Phase				
Model	**Validation Metrics**			
	R^2	**RMSE**	**MSE**	**MAE**
RT	0.3	0.22	0.05	0.16
GPR	0.23	0.20	0.04	0.15
ANN 5-17-7-1	0.46	0.18	0.04	0.12

Table 7. Evaluation of the modeling with testing data among different algorithms: RT, GPR, and ANN.

Test Phase				
Model	**Validation Metrics**			
	R^2	**RMSE**	**MSE**	**MAE**
RT	0.3	0.19	0.04	0.15
GPR	0.27	0.22	0.05	0.17
ANN 5-17-7-1	0.58	0.17	0.03	0.12

6. Conclusions

This study analyzes the influence of industrial grinding process parameters on surface roughness in an industrial setup, comparing MQL and conventional cooling methods. For this purpose, dressing depths of 2, 5, 10, and 20 microns, a tool feed rate ranging from 50 to 600 mm/min, and an attack angle of 10 degrees were employed to establish the grinding wheel cycle. The grinding procedure on the Inconel 738 nickel-based superalloy workpiece involved a cutting speed of 47 m/s, a feed rate ranging from 4.5 to 15 m/min, and a cutting depth of 30 microns. The neural network was trained and evaluated using the generated dataset. The key findings of this study are summarized as follows:

In this study, the ANOVA test highlights the substantial impact of the dresser and cooling method on surface roughness, underlining their sensitivity to a_d. The complexity of surface roughness dynamics is acknowledged, suggesting that relying solely on ANOVA testing may not fully illuminate the complete range of parameter dependencies. This study goes beyond ANOVA-confirmed parameters, considering all relevant factors in the analysis to train an Artificial Neural Network (ANN). Notably, the novelty lies in treating cooling methods and dressers as independent parameters, which contributes to the study's unique level of accuracy and emphasizes the introduction of complexity and variability. The future direction involves improving accuracy through the incorporation of these factors and more advanced algorithms in subsequent research.

The results of the ANOVA analysis revealed a significant correlation between grinding parameters, particularly qualitative parameters such as cooling. However, the analysis indicated that some other parameters, such as the dresser type, do not significantly contribute to the model and could potentially be excluded from the implementation. Despite this, in the literature mentioned in Section 4.2, it is illustrated that in practice, it is not feasible to entirely eliminate these parameters from the grinding process and there are indirect and nonlinear correlations. It is also important to note that the ANOVA process is highly sensitive to data distribution. The data must be normally distributed for ANOVA to function correctly, and the parameters in this study did not sufficiently meet this criterion. Therefore, while ANOVA provides an initial insight into this research, it demonstrates that a purely statistical analysis may not yield a comprehensive and reliable solution for the current study. As such, a more robust approach such as machine learning for further analysis has been proposed in this work.

Furthermore, the study introduces a sophisticated algorithm to establish an optimal network structure for the ANN, considering various transfer functions and neural sizes. The results indicate that a deeper network with two hidden layers using specific transfer functions and neuron sizes is favorable for the available dataset. The ANN algorithm exhibited independence from the quantity of parameters and was found to be versatile

for potential online deployment and broader application across engineering domains. The authors' future research endeavors aim to enhance prediction accuracy, specifically by treating the coolant and dresser as independent parameters. They also intend to use digitized data and models for smart machining via the Industrial Internet of Things (IIoT), seeking to achieve desired surface roughness levels more efficiently.

Appendix A

Table A1. A subset of 12 random data points is taken from the primary dataset for testing of the trained model. The current dataset encompasses a total of 125 data sets for the grinding process.

|	Input Parameters					Output Parameters		
	v_{ft}	v_{fd}	a_d	*Dressing*	*Cooling*	R_z	$R_z(max)$	$R_z(min)$
1	4.5	213	5	1	1	2.4425	2.64	2.36
2	4.5	50	10	1	2	2.37	2.58	2.25
3	15	600	10	1	2	2.2625	2.45	2.11
4	4.5	213	10	4	1	6.585	6.47	5.94
5	15	50	5	4	1	3.36	3.94	3.17
6	15	50	10	4	1	4.175	4.56	3.82
7	15	213	10	4	1	3.39	3.65	3.08
8	4.5	420	5	4	2	3.49	3.77	3.18
9	15	600	10	4	2	4.41	4.69	4.39
10	15	420	20	4	2	3.925	4.39	3.66
11	4.5	50	2	1	1	2.635	2.8	2.56
12	15	600	20	4	1	2.4425	2.64	2.36

Appendix B

(**a**)

(**b**)
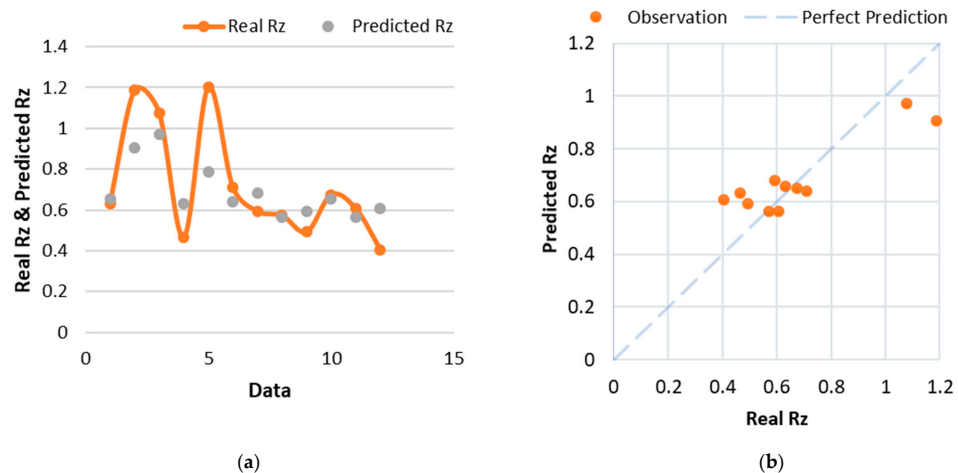
Figure A1. Comparison of the real surface roughness (R_z) against predicted roughness with ANN (**a**). It is noteworthy to observe that the predicted observations from the test data closely match the ideal prediction in (**b**).

Table A2. Analysis of the Artificial Neural Network test data.

Analysis Type	Results
Acc (mean)	82
Acc (std)	15
Acc (MAX)	99
Acc (Min)	51
R	0.865234
R2	0.582239
MSE	0.0296876
RMSE	0.172301
MAE	0.12742
MAPE	17.9083
SMAPE	17.3525

References

1. Puerto, P.; Fernández, R.; Madariaga, J.; Arana, J.; Gallego, I. *Evolution of Surface Roughness in Grinding and Its Relationship with the Dressing Parameters and the Radial Wear*; Elsevier: Amsterdam, The Netherlands, 2013. Available online: https://www.sciencedirect.com/science/article/pii/S1877705813013945 (accessed on 6 October 2022).
2. Pinto, F.W. An Experimental and Numerical Approach to Investigate the Machining Performance of Engineered Grinding Tools. Ph.D. Thesis, ETH Zurich, Zurich, Switzerland, 2008. [CrossRef]
3. Grinding. Haynes International. 2020. Available online: https://www.haynesintl.com/alloys/fabrication-brochure/grinding (accessed on 6 October 2022).
4. The Importance of Material Grinding in Manufacturing—Bright Hub Engineering. 2009. Available online: https://www.brighthubengineering.com/manufacturing-technology/37092-grinding-wheels-and-the-grinding-process/ (accessed on 6 October 2022).
5. Czapiewski, W. Methods of minimalization of coolant flow rate in the grinding processes—The review. *J. Mech. Energy Eng.* **2017**, *1*, 117–122. Available online: https://jmee.tu.koszalin.pl/ojs/index.php/jmee/article/view/27 (accessed on 6 October 2022).
6. Webster, J.A. In Grinding, Coolant Application Matters. 2008. Available online: https://www.sme.org/grinding-coolant-application-matters (accessed on 6 October 2022).
7. Inconel, Inco Alloys, Superalloy, Nickel Based Steel Alloy—Mega Mex. Available online: https://megamex.com/inconel/ (accessed on 6 October 2022).
8. Alloy IN-738 Technical Data. Available online: https://nickelinstitute.org/media/4690/ni_inco_497_alloy738.pdf (accessed on 6 October 2022).
9. Zayegh, A.; Al Bassam, N. Neural network principles and applications. In *Digital Systems*; IntechOpen: London, UK, 2018. [CrossRef]
10. Pai, A. ANN vs. CNN vs. RNN | Types of Neural Networks. 2020. Available online: https://www.analyticsvidhya.com/blog/2020/02/cnn-vs-rnn-vs-mlp-analyzing-3-types-of-neural-networks-in-deep-learning/ (accessed on 6 October 2022).
11. Wimmer, M.; Hartl, R.; Zaeh, M.F. Determination of the Cutting-Edge Microgeometry Based on Process Forces during Peripheral Milling of Ti-6Al-4V Using Machine Learning. *J. Manuf. Mater. Process.* **2023**, *7*, 100. [CrossRef]
12. Marian, M.; Tremmel, S. Current trends and applications of machine learning in tribology—A review. *Lubricants* **2021**, *9*, 86. [CrossRef]
13. Zuo, Y.; Lundberg, J.; Chandran, P.; Rantatalo, M. Squat Detection and Estimation for Railway Switches and Crossings Utilising Unsupervised Machine Learning. *Appl. Sci.* **2023**, *13*, 5376. [CrossRef]
14. Ahmad, R.; Wazirali, R.; Abu-Ain, T. Machine learning for wireless sensor networks security: An overview of challenges and issues. *Sensors* **2022**, *22*, 4730. [CrossRef]
15. Li, C.; Wu, Y.; Li, X.; Ma, L.; Zhang, F.; Huang, H. Deformation characteristics and surface generation modelling of crack-free grinding of GGG single crystals. *J. Mater. Process. Technol.* **2020**, *279*, 116577. [CrossRef]
16. Zhou, H.; Ding, W.F.; Li, Z.; Su, H.H. Predicting the grinding force of titanium matrix composites using the genetic algorithm optimizing back-propagation neural network model. *Proc. Inst. Mech. Eng. Part B J. Eng. Manuf.* **2018**, *233*, 1157–1167. [CrossRef]
17. Unune, D.R.; Mali, H.S. Artificial neural network–based and response surface methodology–based predictive models for material removal rate and surface roughness during electro-discharge diamond grinding of Inconel 718. *Proc. Inst. Mech. Eng. Part B J. Eng. Manuf.* **2015**, *230*, 2081–2091. [CrossRef]
18. Pan, Y.; Wang, Y.; Zhou, P.; Yan, Y.; Guo, D. Activation functions selection for BP neural network model of ground surface roughness. *J. Intell. Manuf.* **2020**, *31*, 1825–1836. [CrossRef]
19. Liu, Y.; Song, S.; Zhang, Y.; Li, W.; Xiao, G. Prediction of Surface Roughness of Abrasive Belt Grinding of Superalloy Material Based on RLSOM-RBF. *Materials* **2021**, *14*, 5701. [CrossRef]
20. Wang, C.; Wang, G.; Shen, C. Analysis and Prediction of Grind-Hardening Surface Roughness Based on Response Surface Methodology-BP Neural Network. *Appl. Sci.* **2022**, *12*, 12680. [CrossRef]

21. Soler, D.; Telleria, M.; García-Blanco, M.B.; Espinosa, E.; Cuesta, M.; Arrazola, P.J. Prediction of surface roughness of SLM built parts after finishing processes using an artificial neural network. *J. Manuf. Mater. Process.* **2022**, *6*, 82. [CrossRef]

22. Buj-Corral, I.; Sender, P.; Luis-Pérez, C.J. Modeling of Surface Roughness in Honing Processes by Using Fuzzy Artificial Neural Networks. *J. Manuf. Mater. Process.* **2023**, *7*, 23. [CrossRef]

23. Szwajka, K.; Zielińska-Szwajka, J.; Trzepieciński, T. The Use of a Radial Basis Function Neural Network and Fuzzy Modelling in the Assessment of Surface Roughness in the MDF Milling Process. *Materials* **2023**, *16*, 5292. [CrossRef]

24. Liu, X.; Pan, Y.; Yan, Y.; Wang, Y.; Zhou, P. Adaptive BP network prediction method for ground surface roughness with high-dimensional parameters. *Mathematics* **2022**, *10*, 2788. [CrossRef]

25. Kanovic, Z.; Vukelic, D.; Simunovic, K.; Prica, M.; Saric, T.; Tadic, B.; Simunovic, G. The modelling of surface roughness after the ball burnishing process with a high-stiffness tool by using regression analysis, artificial neural networks, and support vector regression. *Metals* **2022**, *12*, 320. [CrossRef]

26. Balonji, S.; Tartibu, L.K.; Okokpujie, I.P. Prediction Analysis of Surface Roughness of Aluminum Al6061 in End Milling CNC Machine Using Soft Computing Techniques. *Appl. Sci.* **2023**, *13*, 4147. [CrossRef]

27. Wang, L.; Fu, S.; Wang, D.; Li, X. Surface Quality Evolution Model and Consistency Control Method of Large Shaft Multi-Pass Grinding. *Appl. Sci.* **2023**, *13*, 1502. [CrossRef]

28. Khalaf, A.A.; Hanon, M.M. Prediction of Friction Coefficient for Ductile Cast Iron Using Artificial Neural Network Methodology Based on Experimental Investigation. *Appl. Sci.* **2022**, *12*, 11916. [CrossRef]

29. Wang, Z.; Hou, G.; Zhao, Y.; Sun, J.; Guo, J.; Chen, W. Characterization of residual stresses and grain structure in hot forging of GH4169. *Aerospace* **2022**, *9*, 92. [CrossRef]

30. Xu, L.; Sun, Z.; Ruan, Q.; Xi, L.; Gao, J.; Li, Y. Development Trend of Cooling Technology for Turbine Blades at Super-High Temperature of above 2000 K. *Energies* **2023**, *16*, 668. [CrossRef]

31. Spina, R.; Cavalcante, B. Evaluation of grinding of unfilled and glass fiber reinforced polyamide 6, 6. *Polymers* **2020**, *12*, 2288. [CrossRef] [PubMed]

32. Yang, D.; Guo, Q.; Wan, Z.; Zhang, Z.; Huang, X. Surface roughness prediction and optimization in the orthogonal cutting of graphite/polymer composites based on artificial neural network. *Processes* **2021**, *9*, 1858. [CrossRef]

33. Trzepieciński, T.; Najm, S.M. Application of artificial neural networks to the analysis of friction behaviour in a drawbead profile in sheet metal forming. *Materials* **2022**, *15*, 9022. [CrossRef] [PubMed]

34. Ficko, M.; Begic-Hajdarevic, D.; Cohodar Husic, M.; Berus, L.; Cekic, A.; Klancnik, S. Prediction of surface roughness of an abrasive water jet cut using an artificial neural network. *Materials* **2021**, *14*, 3108. [CrossRef] [PubMed]

35. Awan, M.R.; González Rojas, H.A.; Hameed, S.; Riaz, F.; Hamid, S.; Hussain, A. Machine Learning-Based Prediction of Specific Energy Consumption for Cut-Off Grinding. *Sensors* **2022**, *22*, 7152. [CrossRef]

36. Prabhu, S.; Uma, M.; Vinayagam, B.K. Surface Roughness Prediction Using Taguchi-Fuzzy Logic-Neural Network Analysis for CNT Nanofluids Based Grinding Process. *Neural Comput. Appl.* **2015**, *26*, 41–55. [CrossRef]

37. Hadad, M.; Attarsharghi, S.; Makarian, J.; Mahdianikhotbesara, A. An Experimental Investigation of the Effects of Dressing and Grinding Parameters on Sustainable Grinding of Inconel 738 Used for Automated Manufacturing. *Processes* **2023**, *11*, 2876. [CrossRef]

38. Hadad, M.; Makarian, J. Experimental investigation of the effects of dressing and coolant-lubricant conditions on grinding of Nickel-based superalloy-Inconel 738. *Energy Equip. Syst.* **2021**, *9*, 27–36. [CrossRef]

39. Svozil, D.; Kvasnička, V.; Pospíchal, J. Introduction to multi-layer feed-forward neural networks. *Chemom. Intell. Lab. Syst.* **1997**, *39*, 43–62. [CrossRef]

40. Jierula, A.; Wang, S.; Oh, T.M.; Wang, P. Study on Accuracy Metrics for Evaluating the Predictions of Damage Locations in Deep Piles Using Artificial Neural Networks with Acoustic Emission Data. *Appl. Sci.* **2021**, *11*, 2314. [CrossRef]

41. Kvålseth, T.O. Cautionary Note about R^2. *Am. Stat.* **1985**, *39*, 279–285.

42. Hyndman, R.J. Another Look at Forecast-Accuracy Metrics for Intermittent Demand. *Foresight Int. J. Appl. Forecast.* **2006**, *4*, 43–46.

43. Kim, C.H.; Kim, Y.C. Application of artificial neural network over nickel-based catalyst for combined steam-carbon dioxide of methane reforming (CSDRM). *J. Nanosci. Nanotechnol.* **2020**, *20*, 5716–5719. [CrossRef] [PubMed]

44. Khramenkov, M.; Jersák, J. Effect of the Dressing Process on the Surface Roughness in Cylindrical Grinding of Ti6Al4V Alloy Using Stationary Diamond Dressing Tools. *Manuf. Technol.* **2021**, *21*, 640–646. [CrossRef]